

# EBSD on the Nacre Structure of a Pearl (*Hyriopsis cumingii*) with 100 nm Resolution – Busting a Myth

## Introduction

Nacre of pearls and mollusc shells is a hybrid nano composite of aragonite ( $\text{CaCO}_3$ ) platelets and biopolymers. The colorful luster of nacre is due to the aragonite platelet thickness which is close to the wavelength of visible light. Further, the hybrid composite nanostructure lends nacre extraordinary mechanical properties. The biopolymer component provides flexibility and tensile strength while, the mineral component is essential for high elastic modulus, compressive and bending strength, as well as hardness and abrasive resistance. The fracture toughness of nacre is orders of magnitude higher than that of pure  $\text{CaCO}_3$  (Mayer, 2005, Barthelat, 2010). Due to the large electron penetration depth in nacre at the conventionally used 20 kV acceleration voltage in SEM/EBSD investigations, a spatial resolution in the order of 1 micron has been reported. (Schmahl et al., 2009, Goetz et al., 2009). This is insufficient to resolve nacreous nanostructures. This application note illustrates how the resolution of EBSD data can be significantly enhanced when low acceleration voltage is used.

## Experimental

EBS maps ranging from 100-400 nm resolution of the nacreous structure of a pearl were obtained on a FEG-SEM equipped with an Oxford Instruments **Nordlys** Nano EBSD, **X-Max**® 80 mm EDS detectors and **AZtec**® software. An acceleration voltage of 8 kV was employed for SEM imaging and EBSD mapping was done at 8 and 15 kV respectively.

The pearl was obtained from a culture of the freshwater pearl mussel *Hyriopsis cumingii* from Japan. A calotte was cut from the perfect sphere and the sectioned surface was carefully polished with final colloidal silica polish in a vibratory polisher. They were then coated with a thin layer of carbon.

## Results and Discussion

Figure 1a shows a high magnification backscattered electron image of the cut and polished calotte surface. This section is from near the centre of the pearl showing polygonal grains superimposed with concentric rings. The concentric rings result from incremental spherical growth of the pearl, and they can be attributed to varying amounts of organic material deposited in the nacreous structure during each growth phase. The thickness of each mineralized layer is estimated to be about 0.2  $\mu\text{m}$ . As the aragonite platelets are arranged perpendicular to the radius of the pearl's spherical outer surface, the aspect ratio of the incremental spherical growth layers changes from equiaxed in the centre of the section to elongated towards the rim as seen in the lower magnification images in Figure 1b.

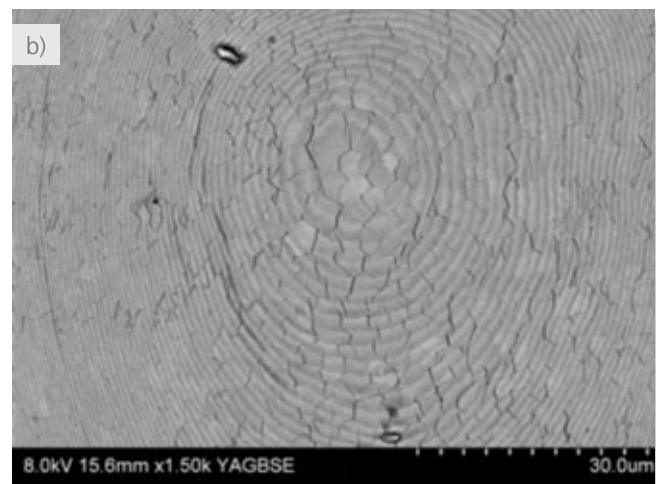
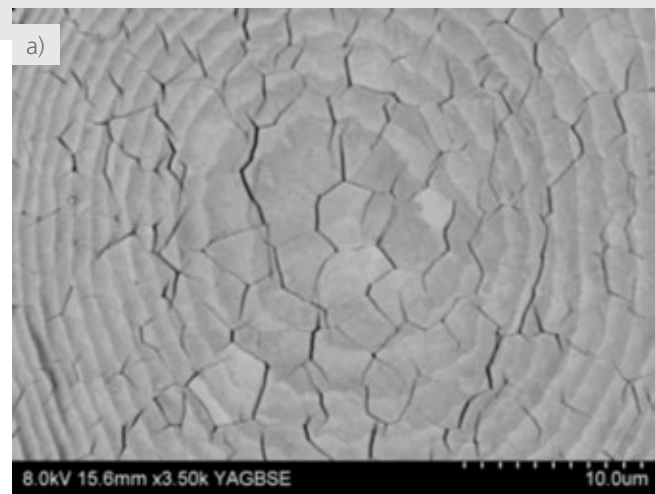


Figure 1. a) and b) backscattered electron images of the cut and polished calotte surface.



The Business of Science®

# EBSD on the Nacre Structure of a Pearl (*Hyriopsis cumingii*) with 100 nm Resolution – Busting a Myth

Figure 2 shows EBSD patterns from nacre collected at 8 and 15 kV. These patterns were indexed with the aragonite match unit which has an orthorhombic structure and lattice parameters  $a=0.496$ ,  $b=7.969$  and  $c=0.574$  nm. A corresponding EDS spectrum shows the main constituents as calcium, carbon and oxygen.

Figure 3 shows an IPF X coloured plus band contrast EBSD map (100 nm step resolution) with a set of corresponding (100) pole figures. The aragonite crystallites have an equiaxed morphology as observed in the SEM image in Figure 1. The growth rings can be seen from the pattern quality map. From the pole figures, it is clear that the platelets have the a-axis in common, which is parallel to the radius vector of the pearl. The aragonite platelets are not hexagonal, not zoned and not internally twinned triplets. This clear EBSD observation puts an end to claims in the literature that aragonite platelets in nacre are typically triply twinned hexagons (Mayer, 2005). The myth originated from the frequently occurring macroscopic hexagonal shaped columns which are triple twins of orthorhombic aragonite crystals.

Figure 4 shows a series of 400 nm step size EBSD band contrast and IPF coloured maps taken at a lower magnification from locations from the 6 mm diameter section of the calotte pearl, as shown in the schematic diagram in Figure 5. As the aragonite platelets are arranged perpendicular to the radius of the pearl's spherical outer surface, the aspect ratio of the plates changes from equiaxed in the centre of the sections, to rectangular. This is clearly observed from the pattern quality maps in Figure 4a. However, the IPF colored maps clearly show that the equiaxed grain structure is maintained with grains migrating across the platelets. From the EBSD pole figures it is evident that the orientation of the a-axes is always perpendicular to the platelets (and parallel to the radius) thus when moving from the centre of the pearl to the rim of the pearl a rotation of the axis of the cylindrical or fibre texture is observed, Figure 4d. Merging the pole figures of all the maps in Figure 4a produces the sum pole figures in Figure 4e, in which the {010} and the {001} pole figures are also shown clearly indicating the rotation of the a axes along the radius of the pearl and the fibre texture about this axis maintained.

An EBSD map acquired from the centre of another calotte is shown in Figure 6. This sample had a thicker carbon coating and so data was acquired at an acceleration voltage of 15 kV. The maps show similar microstructural and crystallographic texture features observed in the data acquired at 8 kV.

## Conclusions

This study is not only the first illustrating successful EBSD characterisation of nacre, but it also puts an end to claims in the literature that aragonite platelets in nacre are typically triply twinned hexagons (Mayer, 2005).

Low KV EBSD has become possible due to significant sensitivity improvements in the NordlysNano detector coupled with Tru-I capability offered in AZtec software, in addition to use of the benefit derived from vibratory polishing for sample preparation.

High-resolution low kV EBSD combined with SEM gives access to a detailed understanding and insight into the of the microstructure of mollusc nacre.

# EBSD on the Nacre Structure of a Pearl (*Hyriopsis cumingii*) with 100 nm Resolution – Busting a Myth

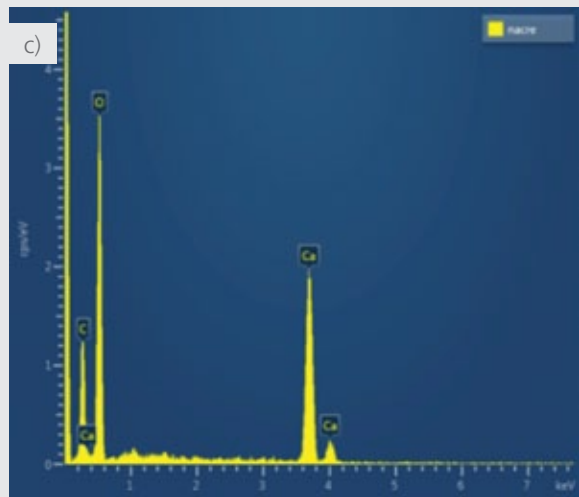
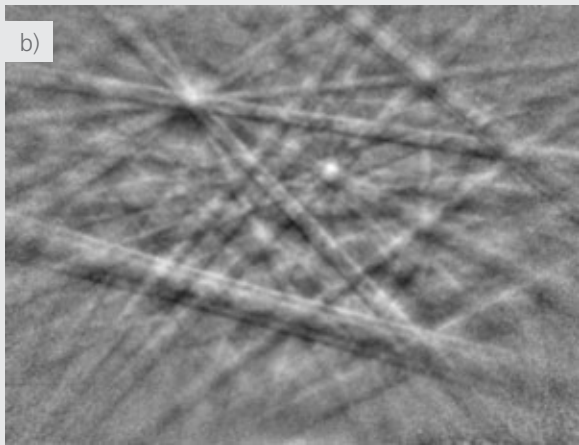
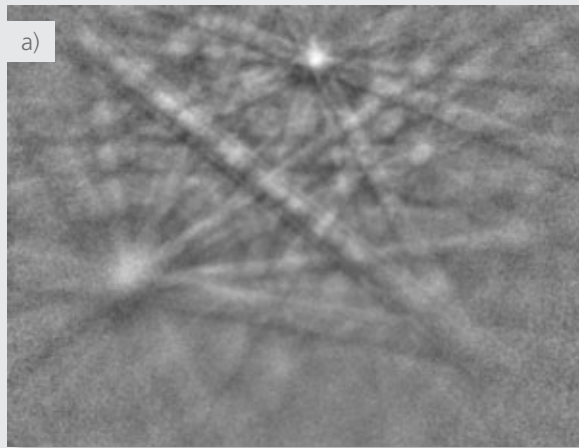


Figure 2. EBSP's from nacre at a) 8 and b) 15 kV and c) corresponding 15 kV EDS spectrum.



Figure 3. a) 8 kV High resolution EBSD IPF X plus pattern quality map from the image in Figure 1b and b) set of scattered pole figures from the map in 3a.

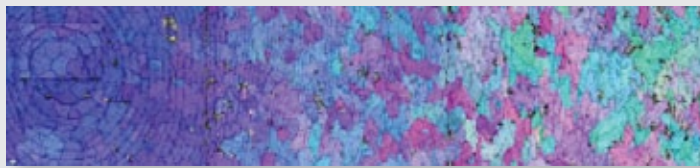
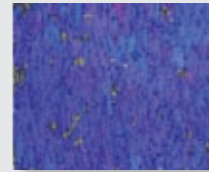
# EBSD on the Nacre Structure of a Pearl (*Hyriopsis cumingii*) with 100 nm Resolution – Busting a Myth



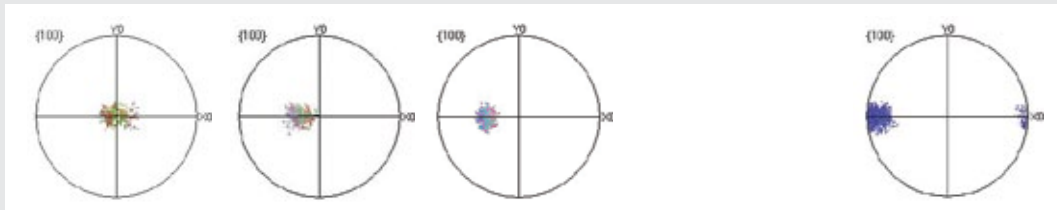
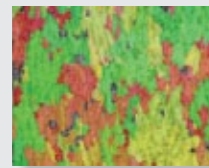
a) band contrast.



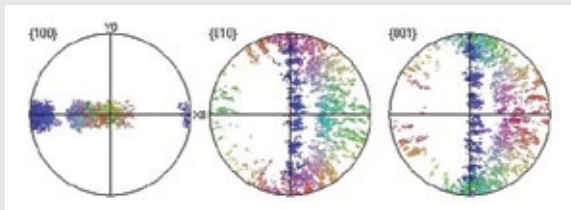
b) IPF X plus band contrast.



c) IPF Z plus band contrast.



d) Scattered {100} pole figures from maps 1, 2, 3 and 4 shown in Figure 4a respectively.



e) Scattered {100}, {010} and {001} pole figures from all maps 1, 2, 3 and 4 shown in Figure 4a.

Figure 4. a-c) EBSD band contrast and IPF coloured maps taken at a lower magnification from locations shown in the schematic diagram 4d d) scattered {100} pole figures from maps 1,2,3 and 4 in Figure 4a and e) scattered {100}, {010} and {001} pole figures from all maps 1,2,3 and 4 in Figure 4a.

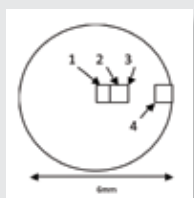


Figure 5. Schematic diagram showing the locations of maps 1,2,3 and 4 where data was collected from the callot.

# EBSD on the Nacre Structure of a Pearl (*Hyriopsis cumingii*) with 100 nm Resolution – Busting a Myth

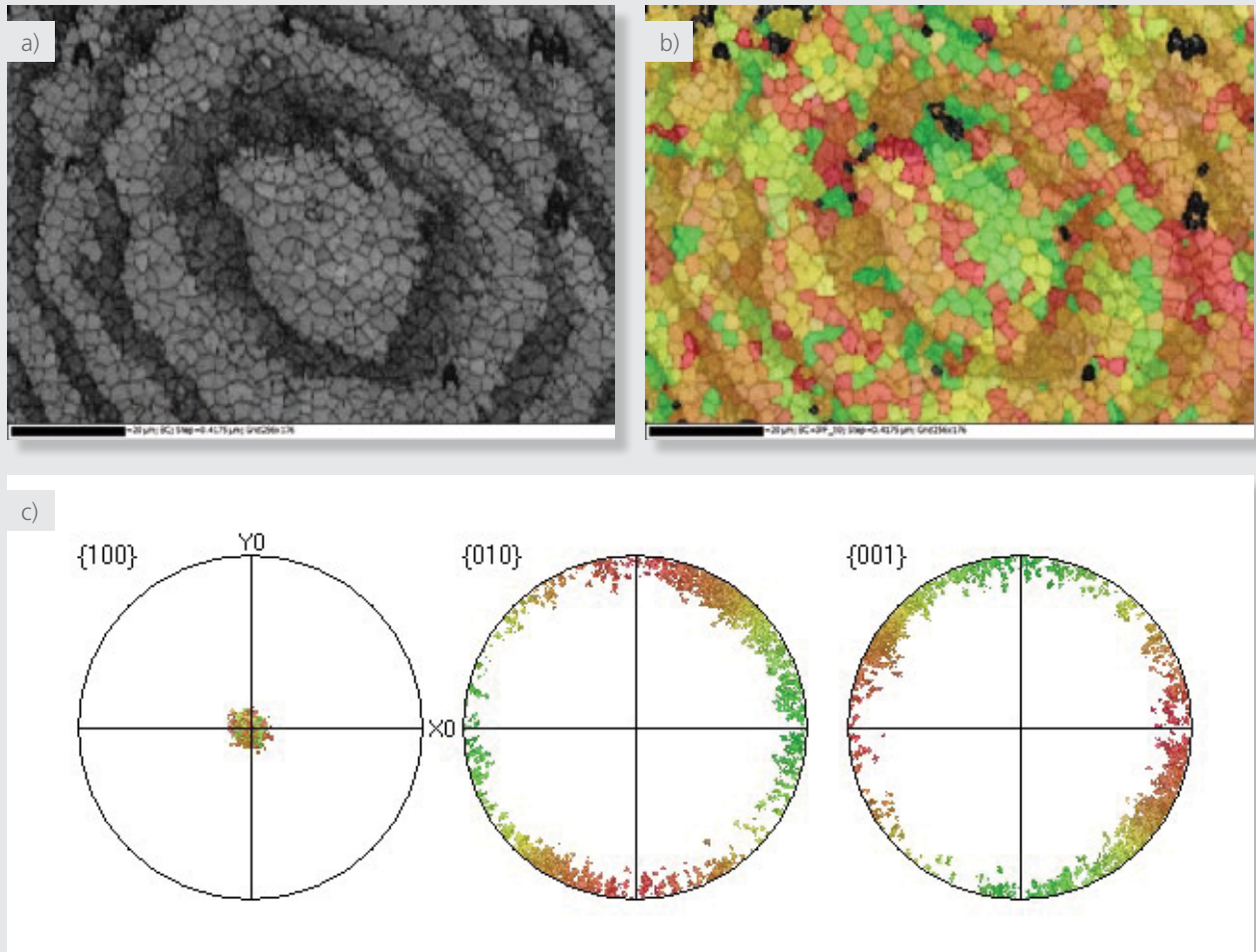


Figure 6. a-b) EBSD band contrast and IPF coloured maps acquired at 15 kV and c) scattered {100} {010} and {001} pole figures.

## References

- G. Mayer (2005) Rigid Biological Systems as Models for Synthetic Composites, *Science* 310, 1144 - 1147
- F. Barthelat (2010) Nacre from mollusc shells: a model for high-performance structural materials.- *Bioinspiration and Biomimetics* 5, 035001
- Schmahl, W.W., Griesshaber, E., Neuser, R.D. Götz, A., Lüter, C. (2009) Electron Back-scatter Diffraction Study of Brachiopod Shell Calcite - Microscale Phase and Texture Analysis of a Polycrystalline Biomaterial.- *Particle & Particle Systems Characterization*, 25, 474-478
- Goetz, A., Griesshaber, E., Neuser, R.D., Luter, C., Hühner, M., Harper, E., Schmahl, W.W. (2009) Calcite morphology, texture and hardness in the distinct layers of rhynchonelliform brachiopod shells.- *Eur. J. Mineral.* 21, 303–315

## Acknowledgements

We thank Dr Erika Griesshaber and Wolfgang W. Schmahl, for this contribution. Dr Griesshaber is grateful for a research grant from the Deutsche Forschungsgemeinschaft (DFG) and would also like to thank Dorrit Jacob, Mainz University, for providing the pearl, Patrick Voss and Dirk Hennemann (BUEHLER GmbH, Düsseldorf) for surface finishing preparation and Mrs. Renate Enders, LMU Munich, for initial preparation.

visit [www.oxford-instruments.com](http://www.oxford-instruments.com) for more information

The materials presented here are summary in nature, subject to change, and intended for general information only. Performances are configuration dependent, and are based on AZtec Release 1.1. Additional details are available. Oxford Instruments NanoAnalysis Quality Management System is certified to meet ISO 9001: 2008. AZtec is a Registered Trademark of Oxford Instruments plc, all other trademarks acknowledged.  
© Oxford Instruments plc, 2011. All rights reserved. Document reference: OINA/EBSD/AN108/0112



*The Business of Science®*